Phase transition and temperature stability of piezoelectric properties in Mn-modified Pb(Mg1/3Nb2/3)O3-PbZrO3-PbTiO3 ceramics

Yongke Yan, Ashok Kumar, Margarita Correa, Kyung-Hoon Cho, R. S. Katiyar, and Shashank Priya

Citation: Applied Physics Letters **100**, 152902 (2012); doi: 10.1063/1.3703124
View online: http://dx.doi.org/10.1063/1.3703124
View Table of Contents: http://scitation.aip.org/content/aip/journal/apl/100/15?ver=pdfcov
Published by the AIP Publishing

Phase transition and temperature stability of piezoelectric properties in Mn-modified $Pb(Mg_{1/3}Nb_{2/3})O_3$-$PbZrO_3$-$PbTiO_3$ ceramics

Yongke Yan,[1,a)] Ashok Kumar,[2] Margarita Correa,[2] Kyung-Hoon Cho,[1] R. S. Katiyar,[2] and Shashank Priya[1,a)]
[1]*Bio-inspired Materials and Devices Laboratory (BMDL), Center for Energy Harvesting Materials and Systems (CEHMS), Virginia Tech, Blacksburg, Virginia 24061, USA*
[2]*Department of Physics and Institute for Functional Nano-materials, University of Puerto Rico, San Juan, Puerto Rico 00931, USA*

(Received 12 October 2011; accepted 22 March 2012; published online 12 April 2012)

This study investigates the effect of two different Mn modifiers [MnO_2 and $Pb(Mn_{1/3}Nb_{2/3})O_3$(PMnN)] on the of phase transitions in $Pb(Mg_{1/3}Nb_{2/3})O_3$-$PbZrO_3$-$PbTiO_3$ ceramics. The temperature dependence of polarization derived from measured pyroelectric current indicated change in nature of phase transition with MnO_2 doping. This phenomenon was supported by the temperature evolution of the linear softening of low lying hard lattice mode as revealed by Raman analysis. The grain size was found to increase with MnO_2 doping (5X) while decrease with PMnN modification (0.5X). Interestingly, the piezoelectric constant of MnO_2 modified composition showed negligible degradation ($<1\%$) even after heat treatment very close to the ferroelectric-paraelectric transition temperature. [http://dx.doi.org/10.1063/1.3703124]

Modified $Pb(Zr,Ti)O_3$ (PZT) based piezoelectric ceramics with combinatory "soft" and "hard" characteristics are required for high power applications. The ideal high power materials should possess high piezoelectric charge coefficient (d), large electromechanical coupling factor (k), large mechanical quality factor (Q_m), and low dielectric loss ($\tan\delta$). In general, adding relaxor type $A(B_1B_2)O_3$ compound (such as $Pb(Mg_{1/3}Nb_{2/3})O_3$ (PMN) and $Pb(Zn_{1/3}Nb_{2/3})O_3$ (PZN)) to PZT enhances the piezoelectric properties (such as d and k) of the material while the acceptor ion (such as Mn^{2+} and Mn^{3+}) increases Q_m and reduces $\tan\delta$.[1–3]

Previously, we have found that MnO_2 doped PMN-PZT and PZN-PZT ceramics exhibit uniform distribution of secondary oxide phase in the perovskite matrix grain structure (MgO secondary phase in MnO_2 doped PMN-PZT and ZnO secondary phase in MnO_2 doped PZN-PZT).[4,5] Taking into account the phase stability of PMN, PZN, and $Pb(Mn_{1/3}Nb_{2/3})O_3$ (PMnN),[6] we have suggested that Mn-ion substitutes on the B-site (such as Mg^{2+}, Zn^{2+}) in order to stabilize the relaxor structure. This results in the complex phase composition corresponding to PMN/PZN-PZT-PMnN matrix with MgO/ZnO secondary phase.[4,5] When $Pb(Mn_{1/3}Nb_{2/3})O_3$ was used instead of MnO_2 as dopant in the PMN-PZT, it was found that the formation of MgO secondary phase was suppressed and the resultant ceramic exhibited constrained grain growth (grain size decreased from $\sim10\,\mu$m to $\sim1\,\mu$m) resulting in improved "hard" property (Q_m increased from 950 to 2060).[4] The combination of these excellent hard characteristics with high temperature stability makes these systems prominent candidate for designing high power devices. However, we also noticed quite interesting phase transition characteristics in this system which was dependent upon the type of Mn-dopant used (MnO_2 or PMnN). In this letter, we investigate the nature of ferroelectric phase transition in the MnO_2 and PMnN modified PMN-PZT ceramics and temperature stability of piezoelectric properties.

Three different compositions were synthesized for this study: (i) $0.4Pb(Mg_{1/3}Nb_{2/3})O_3$-$0.25PbZrO_3$-$0.35PbTiO_3$ (PMN-PZT), (ii) 2 mol. % MnO_2 doped $0.4Pb(Mg_{1/3}Nb_{2/3})O_3$-$0.25PbZrO_3$-$0.35PbTiO_3$ (PMN-PZT + MnO_2), and (iii) $0.06Pb(Mn_{1/3}Nb_{2/3})O_3$-$0.34Pb(Mg_{1/3}Nb_{2/3})O_3$-$0.25PbZrO_3$-$0.35PbTiO_3$ (PMN-PZT + PMnN). Detailed description of the sample preparation can be found elsewhere.[4] The phase and microstructure of sintered samples was examined by x-ray diffraction (XRD, PANalytical X'Pert) and scanning electron microscopy (SEM, FEI Quanta 600 FEG). Dielectric constant (ε_r) and $\tan\delta$ were measured by using a LCR meter (HP4287A). Electromechanical coupling factor (k_{31}) was obtained by using resonance-antiresonance technique through impedance/gain analyzer (HP4194A). Thermally stimulated depolarization current (TDSC) was measured at heating rate of 2 °C/min using pA meter (HP4140B). Impedance spectrum was measured using HP4194A over frequencies from 100 Hz to 15 MHz. Raman spectra were obtained using Jobin-Yvon T64000 Triple spectrometer.

Figure 1 shows the SEM images and corresponding XRD patterns of all three samples. All the compositions exhibited perovskite structure and were close to the morphotropic phase boundary (MPB) as indicated by splitting of (111) and (200) peaks (Fig. 1S of Ref. 7). We expect slight shift in the base composition by Mn-modification as indicated by change in the (111) and (200) peak position and shift in the Curie temperature. The MPB of relaxor based systems is known to be slightly curved thus the shift in the composition towards rhombohedral side for PMN-PZT + MnO_2 will result in lower Curie temperature (Fig. 2S of Ref. 7). The microstructures in Fig. 1 shows the dense sintered body and variation in grain size with the type of Mn-doping ($\sim2\,\mu$m for PMN-PZT, $\sim1\,\mu$m for PMN-PZT-PMnN, and $\sim10\,\mu$m for PMN-PZT + MnO_2). Further, there is precipitation of MgO second phase in PMN-PZT + MnO_2

a)Authors to whom correspondence should be addressed. Electronic addresses: yanthu@gmail.com and spriya@vt.edu.

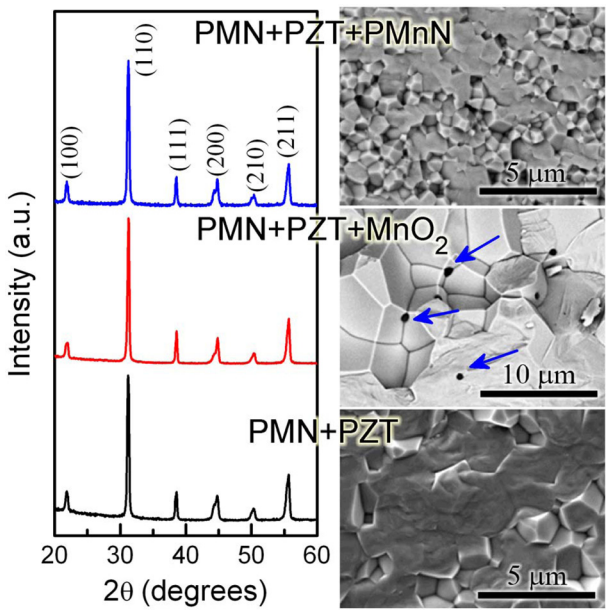

FIG. 1. XRD patterns and SEM images of PMN-PZT, PMN-PZT + MnO_2, and PMN-PZT + PMnN sintered samples.

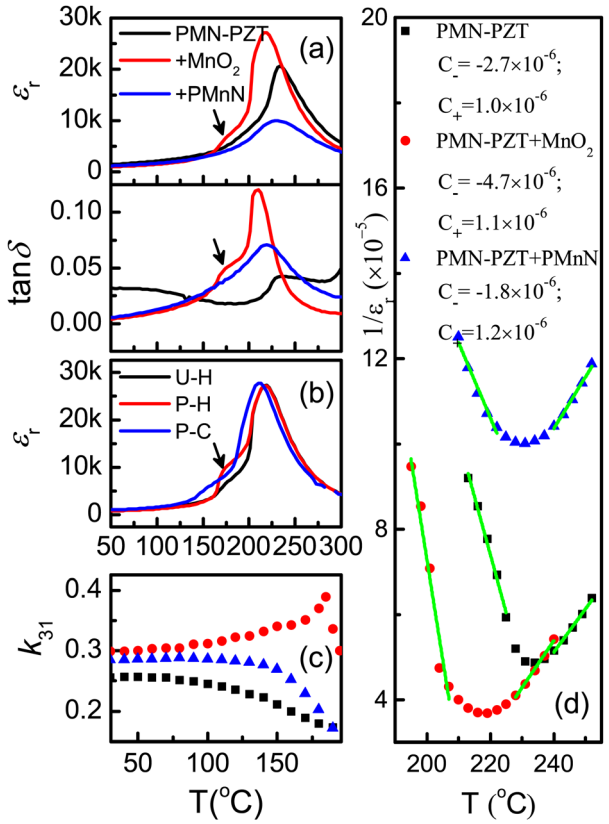

FIG. 2. (a) Dielectric constant and loss as a function of temperature for PMN-PZT, PMN-PZT + MnO_2, and PMN-PZT + PMnN samples at the frequency of 1 kHz. (b) Dielectric constant as a function of temperature for PMN-PZT + MnO_2 under different conditions (U: unpoled, P: poled, H: heating, C: cooling). (c) Electromechanical coupling factor k_{31} as a function of temperature for poled samples. (d) Inverse of dielectric constant as a function of temperature for unpoled samples at the frequency of 1 kHz.

ceramic (EDS/SEM analysis shown in Fig. 3S of Ref. 7), while PMN-PZT-PMnN exhibited single phase normal microstructure. PMnN is more stable than PMN in nonstoichiometric MnO_2 doped PMN-PZT which promotes the chemical reaction given as $3Pb(Mg_{1/3}Nb_{2/3})O_3 + MnO \rightarrow 3Pb(Mn_{1/3}Nb_{2/3})O_3 + MgO$. The secondary phase MgO in MnO_2 doped PMN-PZT accelerates the grain growth by modulating the grain boundary migration energy.

The variation of ε_r and tan δ as a function of temperature for all three samples at the frequency of 1 kHz is shown in Fig. 2(a). All samples exhibited diffuse phase transition near the ε_r maximum (T_m) due to relaxor nature of PMN. The maximum value of ε_r at T_m for PMN-PZT + PMnN ceramic decreased while that of PMN-PZT + MnO_2 increased. Randall *et al.* have shown that grain sizes below critical level results in decreased magnitude at T_m and diffused phase transition.[8] In the case of relaxor PMN-PT, decrease in grain size results in reduction of the dielectric constant at T_m; however, this effect is more prominent as the grain size approaches ~0.1 μm.[9] In another study on $BaTiO_3$, they did not see any shift in T_m until the grain sizes were in submicron range.[10] Thus, changes in dielectric behavior of PMN-PZT + PMnN and PMN-PZT + MnO_2 will have some contribution from the 10X difference in grain size, but other factors are required to explain the overall variation. We did not observe any effect of frequency on the T_{max}, which confirmed that the observed effects were related to composition not space charge polarization (Fig. 4S in Ref. 7). Another interesting observation was the existence of peak of ε_r and tan δ around 170 °C in PMN-PZT + MnO_2, which became sharp for the poled sample as shown in Fig. 2(b). To exclude the possibility of defect dipole relaxation, the ε_r vs. T curves were measured during cooling down (from 350 °C, far above T_m). The dielectric spectrum still exhibits the intermediate peak though with thermal hysteresis. The influence of MgO secondary phase on this intermediate peak can be ruled out since MgO is not ferroelectric and has no phase transition around this temperature. Therefore, the peak around 170 °C should be attributed to phase transition of PMN-PZT + MnO_2 matrix from rhombohedral to tetragonal phase.

To clarify the nature of intermediate phase transition, electromechanical property of three compositions was measured as a function of temperature as shown in Fig. 2(c). The k_{31} of PMN-PZT + PMnN was found to continuously decrease with increasing temperature showing tendency similar to that of unmodified PMN-PZT. On the other hand, the k_{31} of PMN-PZT + MnO_2 gradually increased with increasing temperature and then suddenly dropped at 170 °C. This result suggests that PMnN modified PMN-PZT had second order phase transition like characteristics as that of pure PMN-PZT, while MnO_2 modified composition exhibited first order phase transition like characteristics. The comparison of change in slope ratio (C_-/C_+) of the reciprocal dielectric constant below and above T_m as shown in Fig. 2(d). For PMN-PZT, C_-/C_+ is close to 2, while PMN-PZT + MnO_2 shows C_-/C_+ of about 4. In accordance with the Landau free energy model, this difference in C_-/C_+ value also suggests the shift of ferroelectric phase transition from second order to first order.[11] This change of phase transition may be related to the defect structure present in the material.

To understand the nature of defect chemistry,[12,13] we conducted TSDC measurements using the technique described in Ref. 13. Figure 3(a) shows the TSDC curves for all of the three compositions. Two sharp peaks in the low

temperature regime can be noticed for the composition PMN-PZT + MnO_2. These peaks correspond to the phase transition temperature from rhombohedral to tetragonal ($T_{R\text{-}T}$) and tetragonal to cubic (Tc) phase transition. In the case of PMN-PZT and PMN-PZT + PMnN the peaks were diffused and had much smaller intensity. This result further confirms the change in order of transition in PMN-PZT + MnO_2 ceramics as compared to that of PMN-PZT + PMnN. The question that one can ask is "Why Mn doping is able to impart such modification?" To answer this question we look at the high temperature TSDC regime shown in Fig. 3(b). The peaks at the high temperature TSDC regime shown in Fig. 3(b) are not related to phase transition but only with the underlying defect structure in the material.[14] Diffuse polarization anomaly above Curie temperature could be related to relaxation of inherent defect structure present such as A-site and oxygen vacancies, space charges, and polar heterogeneities due to high temperature processing and balancing of the electroneutrality condition. Recently, Matsudo *et al.* have conducted TSDC measurement on the $Na_{0.5}K_{0.5}NbO_3$ ceramics and have shown that large current anomaly around 370 °C is related to the relaxation of oxygen vacancies.[15] We believe that peak observed in the PMN-PZT is also related to the relaxation of oxygen vacancies ($V_O^{\bullet\bullet}$) [Ref. 15] formed due to evaporation of PbO at high sintering temperature; i.e., $Pb^{2+} + O^{2-} \Longleftrightarrow V''_{Pb} + V_O^{\bullet\bullet} + PbO\uparrow$. The relaxation peaks were suppressed in Mn-doped PMN-PZT samples which could be attributed to two factors: reduction in the evaporation of the PbO and formation of defect complexes. The suppression of oxygen vacancy formation during high temperature processing is well known in La-modified PZT ceramics. The defect association between Mn ion and $V_O^{\bullet\bullet}$ is much stronger than $V''_{Pb} - V_O^{\bullet\bullet}$, because $V_O^{\bullet\bullet}$ formed due to PbO evaporation can be compensated by annealing in oxygen atmosphere, while $V_O^{\bullet\bullet}$ formed by the acceptor Mn ions are thermodynamically stable for the local electrical neutralization. Figure 3(c) shows the change in polarization magnitude obtained by integrating the curve in Fig. 3(a) between room temperature and 400 °C. Noticeably, large magnitude of integrated polarization (int. P) for PMN-PZT reflects the contribution from oxygen vacancies. The significantly reduced magnitude of int. P in Mn modified specimen could be attributed to bound defects requiring high threshold energy for diffusion. The reason for difference in the defect structure of PMnN modified and MnO_2 modified samples could be that MnO_2 doping also introduces microstructural inhomogeneities (formation and distribution of MgO resulting in structural heterogeneities) which scale with the defect structure.

Figure 4(a) shows the impedance spectra of three samples, and a simple R-C fit to the semi-circles was performed to determine the DC conductivity shown in Fig. 4(b). The results illustrate that the resistivity of PMN-PZT increases about 10X by Mn doping. Similar phenomenon was observed in Mn doped $BaTiO_3$ and explained on the basis of low $V_O^{\bullet\bullet}$ and electron/hole trapping effect due to multivalence nature of Mn.[16] This figure also shows that the

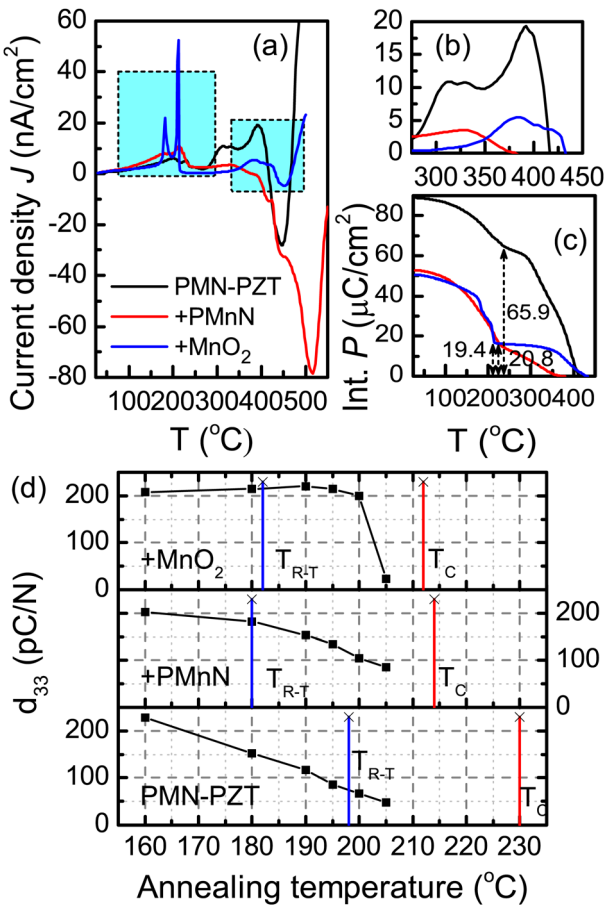

FIG. 3. (a) Thermally stimulated depolarization current (TSDC) of poled PMN-PZT, PMN-PZT + MnO_2, and PMN-PZT + PMnN samples, (b) enlarged windows, (c) room temperature d_{33} as a function of annealing temperature (holding time: 30 min, short circuited, transition temperature $T_{R\text{-}T}$ and T_C recorded from pyroelectric current peaks from Fig. 3(a)).

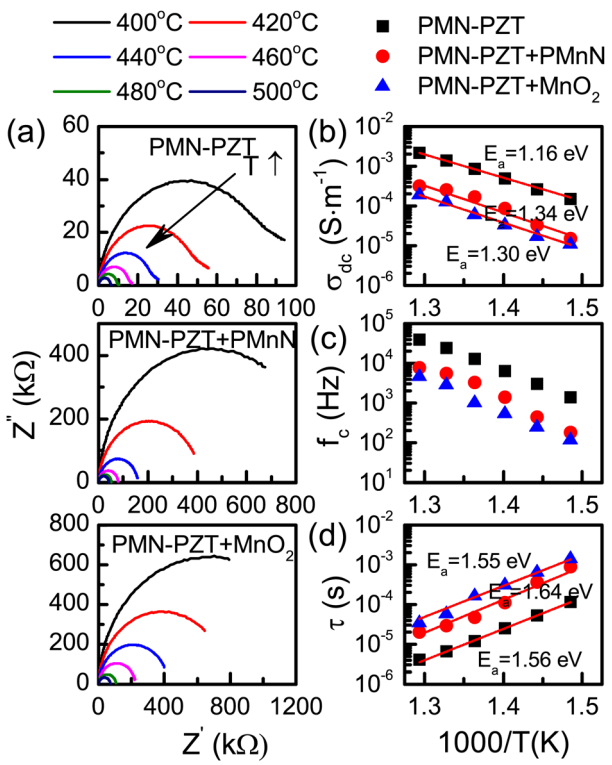

FIG. 4. (a) Impedance spectra of unpoled PMN-PZT, PMN-PZT + PMnN, and PMN-PZT + MnO_2 at different temperature; (b) DC conductivity (σ_{dc}); (c) characteristic frequency (f_c); (d) relaxation time constant (τ) versus inverse temperature for PMN-PZT, PMN-PZT + PMnN, and PMN-PZT + MnO_2.

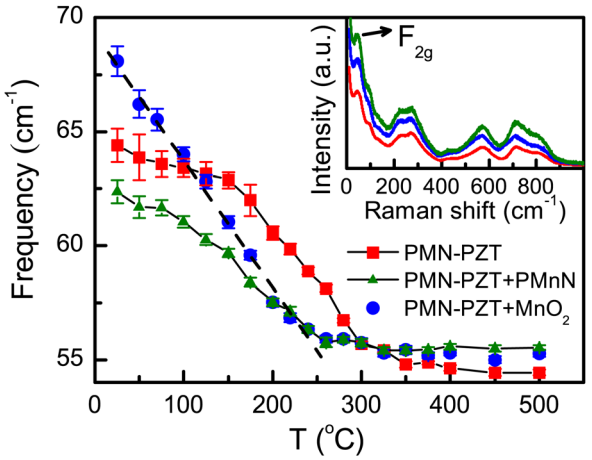

FIG. 5. Frequency of the F_{2g} phonon mode as a function of temperature for PMN-PZT, PMN-PZT + MnO_2, and PMN-PZT + PMnN samples, and inset is room temperature Raman spectra.

resistivity of the PMnN modified samples is lower than that of MnO_2 one, further confirming the contributions arising from the activation of nanoscale heterogeneities. Arrhenius fit to the DC conductivity plot with temperature showed that Mn modified samples had higher activation energy than that of PMN-PZT, which further confirms formation of defect complexes in the Mn-modified specimen. The large difference in the relaxation time (Fig. 4(d)) between the Mn-modified and unmodified sample again indicates that oxygen vacancies are predominantly present as defect complex in the Mn-modified sample.

To further understand the difference in phase transition behavior of MnO_2 doped and PMnN modified PMN-PZT, Raman scattering was employed. Raman spectroscopy is a powerful tool to investigate the local crystal structure, defects, domain dynamics, and phase transition behavior of ferroelectric materials.[17–19] The room temperature Raman spectra of pure PMN-PZT, PMN-PZT-PMnN, and PMN-PZT + MnO_2 are shown in the inset of Fig. 5. The spectra have similar features and they match well with those reported for the complex B-site relaxor ferroelectric family materials.[17–19] It consists of strong phonon modes with peak frequency at ~43, 571, 714, and 814 cm^{-1} plus a band at frequency range of 200–300 m^{-1} and a shoulder at ~95 cm^{-1}. Lowest and intermediate phonon modes showed anomalous behavior with temperature, the complete details of the temperature evolution of the phonon modes will be presented elsewhere. The low frequency (~43 cm^{-1}) hard lattice mode is of special interest to investigate the ferroelectric phase transition.[17] The temperature-dependence of the frequency of this mode for the different samples is shown in Fig. 5. This mode is assigned as F_{2g} mode, and it is associated with the Pb-O stretching vibration; the details of phonon fitting routine can be found in Ref. 17. The frequency of the F_{2g} mode decreases on increasing temperature for pure and doped PMN-PZT samples, but when the transition temperature is reached, the frequency remains almost constant. PMN-PZT and PMN-PZT + PMnN samples exhibited smooth and continuous change in frequency of about ~7 cm^{-1} while PMN-PZT + MnO_2 showed a linear and sharp decrease of about ~11 cm^{-1}. This anomalous behavior of phonon softening further supports a phase transition of second order for the former compositions and first order for the later.

The variation of transition behavior affects the temperature stability of piezoelectric properties. Despite of having higher T_m, PMN-PZT and PMN-PZT-PMnN ceramics showed about 70% and 50% respective decrease in piezoelectric coefficient d_{33} (Fig. 3(d)). However, PMN-PZT + MnO_2 exhibited almost negligible degradation (<1%) after heat treatment at 200 °C. It demarcates two types of Mn-modified samples and indicates the stable nature of piezoelectric response in the MnO_2 modified case. This excellent temperature stability of electromechanical property of PMN-PZT + MnO_2 has huge relevance for high power application which can be associated with the narrow phase transition range.

In summary, this study shows that two different Mn modifiers [MnO_2 and PMnN] have different impact on the phase transition of PMN-PZT piezoelectric ceramics. MnO_2 doping changes phase transition from second order to first order. This phenomenon was supported by the temperature evolution of the low frequency hard lattice mode as revealed by Raman analysis. It is suggested that the MnO_2 modification facilitated the ferroelectric long-range ordering and higher temperature stability of piezoelectric properties.

The authors gratefully acknowledge the financial support from DARPA Heterostructural Uncooled Magnetic Sensors (HUMS) program and Office of Basic Energy Science, Department of Energy. The authors would like to sincerely thank Clive Randall for helpful discussions and suggestions.

[1]S. Priya, K. Uchino, J. Ryu, C. W. Ahn, and S. Nahm, Appl. Phys. Lett. **83**, 5020 (2003).
[2]R. A. Islam, S. Priya, and A. Amin, J. Mater. Sci. **42**, 10052 (2007).
[3]H. Y. Park, C. H. Nam, I. T. Seo, J. H. Choi, S. Nahm, H. G. Lee, K. J. Kim, and S. M. Jeong, J. Am. Ceram. Soc. **93**, 2537 (2010).
[4]Y. Yan, K.-H. Cho, and S. Priya, J. Am. Ceram. Soc. **94**, 4138 (2011).
[5]Y. Yan, K.-H. Cho, and S. Priya, J. Am. Ceram. Soc. **94**, 3953 (2011).
[6]N. Wakiya, K. Shinozaki, and N. Mizutani, J. Am. Ceram. Soc. **80**, 3217 (1997).
[7]See supplementary material at http://dx.doi.org/10.1063/1.3703124 for Figs. S1-S4.
[8]C. A. Randall, N. Kim, J.-P. Kucera, W. Cao, and T. R. Shrout, J. Am. Ceram. Soc. **81**, 677 (1998).
[9]C. A. Randall, A. D. Hilton, D. J. Barber, and T. R. Shrout, J. Mater. Res. **8**, 880 (1993).
[10]D. McCauley, R. E. Newnham, and C. A. Randall, J. Am. Ceram. Soc. **81**, 979 (1998).
[11]A. Kumar, N. M. Murari, and R. S. Katiyar, Appl. Phys. Lett. **90**, 262907 (2007).
[12]S. H. Yoon, C. A. Randall, and K. H. Hur, J. Am. Ceram. Soc. **93**, 1950 (2010).
[13]W. Liu and C. A. Randall, J. Am. Ceram. Soc. **91**, 3245 (2008).
[14]B. S. Kang, S. K. Choi, and C. H. Park, J. Appl. Phys. **94**, 1904 (2003).
[15]H. Matsudo, K. Kakimoto, and I. Kagomiya, Jpn. J. Appl. Phys. **49**, 09MC07 (2010).
[16]S. H. Yoon, C. A. Randall, and K. H. Hur, J. Appl. Phys. **108**, 064101 (2010).
[17]M. Correa, A. Kumar, S. Priya, R. S. Katiyar, and J. F. Scott, Phys. Rev. B **83**, 014302 (2011).
[18]I. G. Siny, S. G. Lushnikoy, R. S. Katiyar, and E. A. Rogacheva, Phys. Rev. B **56**, 7962 (1997).
[19]B. Mihailova, B. Maier, C. Paulmann, T. Malcherek, J. Ihringer, M. Gospodinov, R. Stosch, B. Guttler, and U. Bismayer, Phys. Rev. B **77**, 174106 (2008).